



## Effect of Simulated Pulpal Pressure on Durability of Microtensile Bond Strength of a Universal Adhesive

Komdao Termkleebuppa\*, Pisol Senawongse and Pipop Saikaew

Department of Operative Dentistry and Endodontics, Faculty of Dentistry, Mahidol University, Bangkok, Thailand

\*Corresponding author, E-mail: komdao.t@gmail.com

### Abstract

This study aimed to evaluate the effects of simulated pulpal pressure on the durability of microtensile bond strength ( $\mu$ TBS) and analyze the micro-morphological structure of the resin-dentin interface of dentin treated with Single Bond Universal; a universal adhesive.

Dentin discs were prepared from forty extracted human mandibular third molars by cutting above and below the CEJ 2 mm into the tooth segment model with 1 mm remaining dentin thickness. The bonding and resin composite placement processes were done under 2 different conditions between a group using a simulated pulpal pressure device (Simulated pulpal pressure: S) and a group without a simulated pulpal pressure device (Non-simulated pulpal pressure: N). The bonded specimens were longitudinally sectioned into the sticks with dimensions approximately  $1 \times 1 \text{ mm}^2$ . Two sticks obtained from the center of each specimen were used for  $\mu$ TBS testing with different conditions: immediate testing ( $n=10$ ) and testing after the 10,000-cycles thermocycling process ( $n=10$ ). The failure mode of the fractured specimens was observed under a scanning electron microscope (SEM). The remaining slabs were further stained with silver nitrate, embedded, and polished for resin-dentin interface observation under the SEM. The data were analyzed using the 2-way ANOVA at the 95% significant level with SPSS software.

The NI group presented the highest  $\mu$ TBS values ( $30.15 \pm 3.08 \text{ MPa}$ ) follow by the SI group ( $25.96 \pm 3.90 \text{ MPa}$ ), NT group ( $25.25 \pm 2.44 \text{ MPa}$ ), and ST group ( $22.47 \pm 1.75 \text{ MPa}$ ) ( $p < 0.05$ ). The failure mode of all testing groups was an adhesive failure, in which the S group showed a fracture pattern at the top of the adhesive layer while the N group was broken at the bottom of the adhesive layer. The study of the resin-dentin interface revealed that the thickness of the hybrid layers ranged from  $0.94\text{-}1.02 \text{ }\mu\text{m}$ . The deposition of silver nitrate particles in the immediate testing group was presented both in SI and NI groups. After the thermocycling process, more accumulation of silver nitrate was observed in both ST and NT groups. In conclusion, the  $\mu$ TBS values and nanoleakage of resin-dentin interface obtained from Single Bond Universal could be affected by simulated pulpal pressure and 10,000-cycle thermocycling process.

**Keywords:** *Simulated Pulpal Pressure, Microtensile Bond Strength, Universal Adhesive, Single Bond Universal*

### 1. Introduction

The universal adhesive is the most modern innovation of dental adhesive that has been developed for bonding between dental materials and tooth structure (Rosa, Piva, & Silva, 2015). It is designed to be used in multimode systems such as etch-and-rinse, self-etching, and selective etching mode. Besides, it is also designed for both direct and indirect restoration depending on the need of the dentist (Sofan et al., 2017). However, the compositions of universal adhesives such as acidic monomer, water, ethanol, acetone, and silane coupling agent conduct these universal adhesives perform more hydrophilicity than other adhesives (Van Landuyt et al., 2007).

Two limitations of hydrophilic adhesive systems are difficulty in elimination of water from adhesives and water attraction. Though evaporation is successful, water may be suddenly diffuse back from the dentin into the adhesive layer (Tay, Pashley, Yiu, Sanares, & Wei, 2003).

Not only the water contained in the adhesive solutions can affect the quality of the bond, but also dentinal fluid as well (Sauro et al., 2007). The presence of retained solvent and the movement of dentinal fluids may cause the incompleting penetration of the resin into the collagen fibrils. Water sorption from dentin may increase the elastic buffering effect of the adhesives that impair the bond strength value (Pashley & Tay, 2001).

The bond strength is amplified as the initial mechanical load to break the cross-sectional area of the bond. Nonetheless, the bond strength is used for giving the prognosis of clinical performance and longevity of the restorations of dental restoration (Oilo, 1993).



## 2. Objectives

The objectives of this study were to evaluate the effects of simulated pulpal pressure on the durability of microtensile bond strength ( $\mu$ TBS) and investigate the micro-morphological structure of the resin-dentin interfaces of dentin treated with Single Bond Universal. There were two null hypotheses in this study. First, the  $\mu$ TBS of a universal adhesive bond to dentin was not affected by the simulation of pulpal pressure. Secondly, the  $\mu$ TBS of a universal adhesive bond to dentin was not affected by the thermocycling as an aging process.

## 3. Materials and Methods

### 3.1 Preparation of specimens

Forty extracted sound human mandibular third molars, kept in 0.1% thymol solution (M Dent, Bangkok, Thailand) at 4°C, were used within six months after the extraction. The protocol was approved by the Faculty of Dentistry/Faculty of Pharmacy, Mahidol University Institutional Review Board, Thailand.

A dentin disc with a remaining dentin thickness of approximately 1.0 mm was prepared by 2 parallel cutting using a slow-speed diamond saw (Isomet, Buehler Ltd, Lake Bluff, IL, USA) under a water coolant. The first cut was 2 mm above the cemento-enamel junction (CEJ) and the second was 2 mm below the CEJ and parallel to the first cut as shown in Figure 1. All pulpal tissues were removed by surgical tweezers without destroying the pre-dentin surface on the pulp chamber wall. The pulp chamber was purified by 2.5% sodium hypochlorite solution (M Dent, Bangkok, Thailand) for 30 s then neutralized chemical reaction of sodium hypochlorite by soaking in distilled water for 30 min (Hosaka et al., 2007). The forty dentin discs without enamel remaining on the occlusal surface were obtained. To create a standard smear layer, each disc was further wet-polished with a 600-grit silicon carbide paper (Buehler, Buehler Ltd., Lake Bluff, IL, USA) for 60 s. Then, the polished specimens were rinsed with distilled water for 5 s before the bonding process (do Amaral et al., 2009; Ferrari, Goracci, Sadek, Eduardo, & Cardoso, 2002).

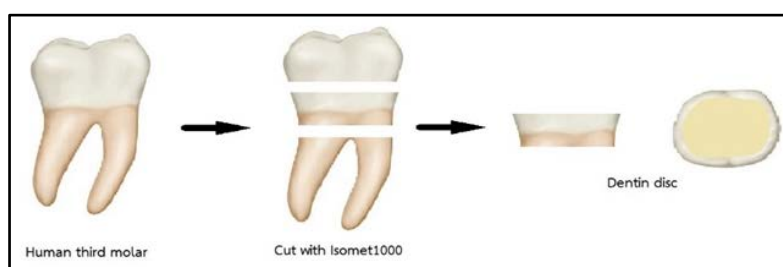


**Figure 1.** Specimen preparation with a slow-speed diamond saw

### 3.2 Experimental design

The polished specimens were randomly divided into 2 major groups depending on the situation of simulated pulpal pressure:

3.2.1 Group S: bonding process was done under the simulated pulpal pressure device, n=20

3.2.2 Group N: bonding process was done without the simulated pulpal pressure device, n=20

Then, the bonded specimens in each group were further divided into two subgroups subjected to either the microtensile testing with an immediate testing group (I) that were tested after 24 h storage in water or the testing after thermocycling group (T) that were tested after artificial aging by thermocycling for 10,000 cycles.

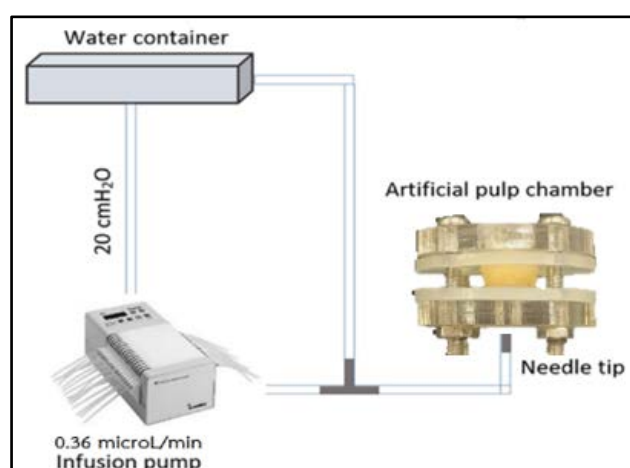
The chemical compositions of the dental adhesive are shown in Table 1.

**Table 1** Chemical compositions, pH, and manufacturer's instruction of the adhesive used in this study

Adhesives	Chemical composition	pH	Application
Single Bond Universal (3M ESPE, St.Paul, MN, USA)	10-MDP, Dimethacrylate resins, HEMA, Vitrebond™ Copolymer, Filler, Ethanol, Water, Photoinitiators, Silane	2.7	1. Apply and rub adhesive for 20 s on dentin 2. Gently air dry for 5 s 3. Light cure for 10 s

### 3.3 Bonding strategies

A specimen in the S group was fixed to a custom-made pulpal chamber then connected for simulating pulpal pressure with an infusion pump (ISMATEC®, Wertheim, Germany) that contained distilled water as shown in Figure 2 (Arsathong K., 2020). The hydraulic pressure was set up to 20 cm H<sub>2</sub>O, and the flow rate was controlled at 0.36  $\mu$ L/min to simulate the intrapulpal pressure and pulpal blood flow rate, consequently (Ciucchi, Bouillaguet, Holz, & Pashley, 1995). While the specimen in the N group was bonded independently without simulated intrapulpal pressure. Single Bond Universal (3M ESPE, St.Paul, MN, USA) was applied onto every specimen following the manufacturer's instruction then cured using LED light-curing unit (LED Bluephase; Ivoclar Vivadent, Schaan, Liechtenstein) with the power intensity of approximately 1,200 mW/cm<sup>2</sup> at a distance of 2 mm from the bonding surface, contacting to the upper acrylic plate of artificial pulp chamber. The distance of the light-curing tip was designed in order to imitate the clinical situation.

**Figure 2** Schematic of hydraulic conductance model using in this study

### 3.4 Resin composite built-up

After light curing, the resin composite Filtek Z350XT (3M ESPE Dental Products Division, St.Paul, MN, USA) was placed onto the bonded surface. Two 2-mm-thick layers of resin composite were placed and cured using the LED light-curing unit (LED Bluephase; Ivoclar Vivadent, Schaan, Liechtenstein) for 40 s.

All bonded specimens were kept in 37°C distilled water for 24 h (Shafiei, Kiomarsi, & Alavi, 2011). After that, all specimens were longitudinally sectioned with a slow-speed diamond blade under a water coolant (Isomet, Buehler Ltd, Lake Bluff, IL, USA) in mesiodistal and buccolingual directions to obtain slab-shaped specimens (Armstrong et al., 2017) as shown in Figure 3. The diameter of each bonded interface of each specimen was gauged with a digital caliper (Mitutoyo, Tokyo, Japan) to a size of approximately 1.0x1.0 mm<sup>2</sup>. The 2 central trimmed specimens of each tooth were subjected to the  $\mu$ TBS test, and the mean of  $\mu$ TBS was calculated to represent the representative bond strength of that tooth. The remaining slabs of specimens were further subjected for the observation of the resin-dentin interface under a scanning electron microscope (SEM).



### 3.5 Aging strategy

Ten specimens (20 sticks) from each group were subjected to the  $\mu$ TBS test after a 24-hour-kept in water. The remaining 10 specimens (other 20 sticks) from each group were subjected to thermocycling (TC400, King Mongkut's Institute of Technology, Ladkrabang, Bangkok, Thailand) for 10,000 cycles in water between 5 and 55°C with a dwell time of 20 s in each water bath and a transfer time of 5 s (Armstrong et al., 2017; Nikaido et al., 2002). This method was applied to simulate the physical degradation process by the aging of the resin-dentin interface.

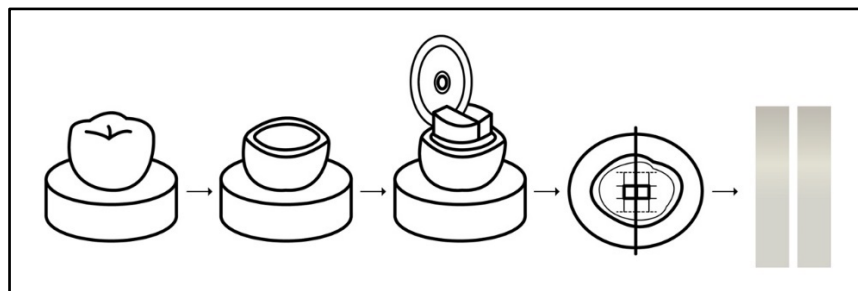


**Figure 3** Reveal the cutting direction of the specimen into sticks

### 3.6 Microtensile bond strength test

For evaluation of  $\mu$ TBS, both non-aging and aging specimens were attached to the  $\mu$ TBS testing jig with cyanoacrylate glue (Model Repair II Blue, Dentsply, SANKIN, Tokyo, Japan) as shown in Figure 4 (Armstrong et al., 2017; Nikaido et al., 2002). Then, the  $\mu$ TBS test was performed with a universal testing machine (Lloyd<sup>TM</sup> Testing Machine, Model LR 10K, Lloyd Instruments, Fareham Hanth, UK) with a 1kN load-cell at a 1.0 mm/min crosshead speed (Chen et al., 2015; Nikaido et al., 2002). The data were calculated and shown in MPa ( $\text{N}/\text{mm}^2$ ).

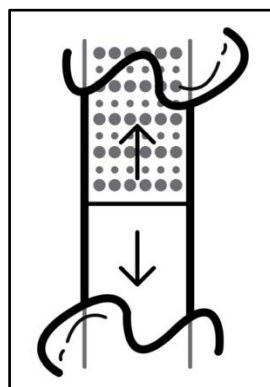


**Figure 4** Exhibit experimental specimen attached to the microtensile bond strength jig with cyanoacrylate glue

### 3.7 Failure mode observation

Each fractured specimen after  $\mu$ TBS testing was identified the failure mode under a light stereomicroscope (Nikon SMZ1000, Nikon; Kanagawa, Japan) at 40x magnification and a scanning electron microscope (JSM-6110 LV, JEOL, Tokyo, Japan) at 70x magnification. The failure modes were classified into 5 types (Flury, Peutzfeldt, & Lussi, 2014); (1) adhesive failure at the dentin-adhesive interface, (2) adhesive failure at the adhesive-resin composite (both type (1) and (2) present 80–100% of the failures occurred at the resin-dentin bond interface), (3) cohesive failure in the dentin (80–100% of the failures



occurred in the underlying dentine), (4) cohesive failure in the resin composite (80–100% of the failures occurred in the overlying composite), and (5) mixed failure (mixed with adhesive failure between the resin and dentin, and cohesive failure in resin and/or dentin) (Senawongse, Srihanon, Muangmingsuk, & Harnirattisai, 2010; Vongphan, Senawongse, Somsiri, & Harnirattisai, 2005).

### 3.8 Observation of micromorphology of the resin-dentin interface under SEM

Resin-dentin slabs from each group were investigated the resin-dentin interface under the SEM (JSM-5410 LV, JEOL, Tokyo, Japan) at 15kV and 20 mm work distance. Each slab was prepared by immersing in 50% silver nitrate solution (pH 7) for 24 h at 37°C. Then, it was subsequently soaked in a photo-developing solution for 8 h under fluorescent light to convert the tracer into metallic silver. Each tracer-infused specimen was soaked in fixer solution for 2 min. After that, the slab was soaked in 10% buffered formalin for 24 h, rinsed with distilled water, and embedded in the epoxy resin. The specimens were polished with 600-, 800-, 1000-, 1500-, 2000-, 3000-, 4,000-, and 5,000-grit SiC papers and 3 $\mu$ , 1 $\mu$ , and 0.25  $\mu$  of diamond paste, subsequently. Consequently, half of the polished specimens were attached to the specimen mount by specific glue. The polished specimens were treated with the argon-ion beam (Cross Section Polisher™ IB-19500CP, JEOL Ltd., Tokyo, Japan) under the condition of 6kV for 12 min.

All specimens were then coated with palladium (K500X Sputter coater, SPI Supplies, West Chester, PA, USA) and observed under the SEM (Niyomsujarit, Senawongse, & Harnirattisai, 2019; Saikaew, Matsumoto, Chowdhury, Carvalho, & Sano, 2018). The investigating was performed using a secondary electron mode (Chen et al., 2015).

The nanoleakage by silver staining at resin-dentin interfaces was observed in the specimens preparing without argon-ion beam etching. For the evaluation of the thickness of the hybrid layer, the specimens with argon-ion beam etching were used for investigation.

### 3.9 Statistical analysis

#### 3.9.1 Microtensile bond strength

The means and standard deviations of the  $\mu$ TBS were calculated. There were 2 factors involving in the  $\mu$ TBS; the situation of simulated pulpal pressure and the aging strategies. All data were organized and analyzed the distribution and homogeneity of variance using the Kolmogorov-Smirnov test and Levene's test respectively. All data showed a normal distribution and homogeneity of variance, and two-WAY ANOVA and multiple comparisons with Duncan were used for further analysis.

#### 3.9.2 Failure mode

The data of failure modes were statistically analyzed using the nonparametric Kruskal-Wallis test.

#### 3.9.3 Resin-dentin interfaces

Descriptive analysis was used for the interpretation of the SEM images of the resin-dentin interface.

All analyses were performed using the SPSS program. A statistical significance was considered to be  $p < 0.05$ .

## 4. Results and Discussion

### 4.1 Microtensile bond strength test

The  $\mu$ TBS values and standard deviations of all experimental groups are demonstrated in Table 2. The normal distribution and equality of variances of all data were analyzed with the Kolmogorov-Smirnov test and Levene's test, respectively. Two-way ANOVA and Duncan were used at a 95% statistically significant level.



**Table 2** Exhibits the mean  $\mu$ TBS value  $\pm$  standard deviations. Groups with the same superscripts are not statistically significant ( $p>0.05$ ).

	Microtensile bond strength (MPa)	
	Immediate testing (I)	After 10,000-cycle thermocycling (T)
<b>Simulated pulpal pressure (S)</b>	25.96 $\pm$ 3.90 <sup>a</sup>	22.49 $\pm$ 1.75 <sup>b</sup>
<b>Non-simulated pulpal pressure (N)</b>	30.15 $\pm$ 3.08 <sup>c</sup>	25.25 $\pm$ 2.44 <sup>a</sup>

According to Table 2, the simulated pulpal pressure device affected the  $\mu$ TBS values of both non-aging and aging groups. For the immediate testing group, the mean  $\mu$ TBS value of the NI group (30.15 $\pm$ 3.08 MPa) was significantly higher than the SI group (25.96  $\pm$  3.90 MPa) ( $p=0.023$ ). While the mean  $\mu$ TBS value after 10,000-cycle thermocycling of the NT group (25.25  $\pm$  2.44 MPa) was significantly higher than the ST group (22.49  $\pm$  1.75 MPa) ( $p=0.009$ ).

The mean  $\mu$ TBS value was also affected by the 10,000-cycle thermocycling process. For the simulated pulpal pressure group, the mean immediate  $\mu$ TBS (25.96 $\pm$ 3.90 MPa) was significantly higher than the aging group (22.49 $\pm$ 1.75 MPa) ( $p=0.023$ ). In accordance with the group without simulated pulpal pressure, the immediate  $\mu$ TBS (30.15 $\pm$ 3.08 MPa) was significantly higher than the aging group (25.25 $\pm$ 2.44 MPa) ( $p=0.001$ ).

#### 4.2 Failure mode observation

All tested specimens in the SI and ST group demonstrated 100% adhesive failure at the adhesive-resin composite interface (Figure 5). The dentin side of specimens was completely covered with adhesive, and the dentinal tubules could not be detected. All those specimens in the NI and NT group expressed 100% adhesive failure at the dentin-adhesive interface (Figure 6). The dentin side of specimens was not covered with adhesive, and the dentinal tubules were filled with resin tags. Therefore, there was no significant difference in the mode of failure among each experimental group, not only in the simulated pulpal pressure group but also in the non-simulated pulpal pressure group ( $p=1.00$ ). However, the group with the different pulpal pressure situation demonstrated a statistically significant difference in the mode of failure ( $p<0.001$ ).

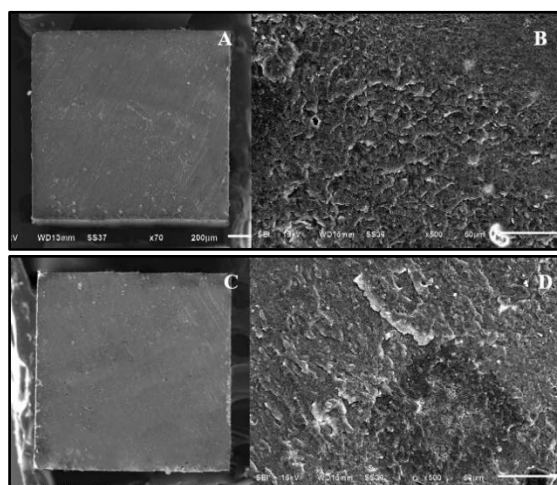


**Figure 5** The representative specimens of the characteristic of adhesive failure at the adhesive-resin composite interface under SEM; 70x resin composite side (A), 500x resin composite side (B), 70x dentin side (C), and 500x dentin side (D).

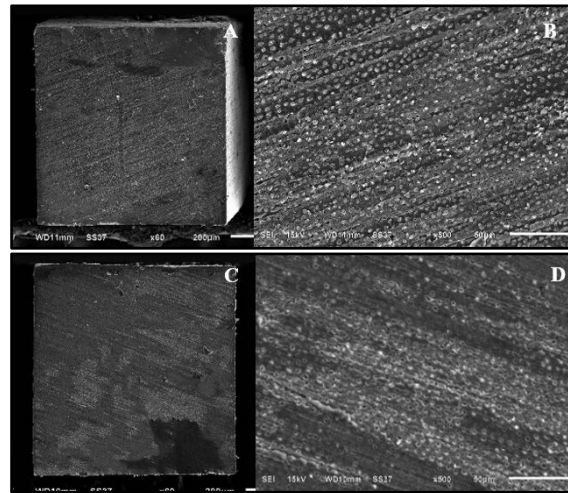


**Figure 6** The representative specimens of the characteristic of adhesive failure at the dentin-adhesive interface (under SEM; 70x resin composite side (A), 500x resin composite side (B), 70x dentin side (C), and 500x dentin side (D)).

#### 4.3 Observation of micromorphology of the resin-dentin interface under SEM

The SEM images of the resin-dentin interfaces for all experimental conditions are shown in Figures 7 and 8. The thickness of the hybrid layer obtained from each experimental group was measured by the ImageJ program, which showed that the SI had the thickness of the hybrid layer approximately  $1.0\ \mu\text{m}$  (Figure 7A) with plenty of silver nitrate deposition along the bottom of the resin-dentin interface (Figure 7B). The ST had  $0.95\ \mu\text{m}$  thickness of the hybrid layer (Figure 7C) with more silver nitrate deposition at the bottom of the hybrid layer than the SI (Figure 7D). Moreover, the water-tree pattern of nanoleakage could be detected at the interface of the SI (asterisk in Figure 7C).

For the groups without simulating the pulpal pressure process, the thickness of the hybrid layer of the NI was approximately  $0.98\ \mu\text{m}$  (Figure 8A) with some silver nitrate deposition at the resin-dentin interface (Figure 8C). The NT had a  $1.00\ \mu\text{m}$  thickness of the hybrid layer (Figure 8B) with more silver nitrate deposition along the bottom of the hybrid layer than the NI (Figure 8D).

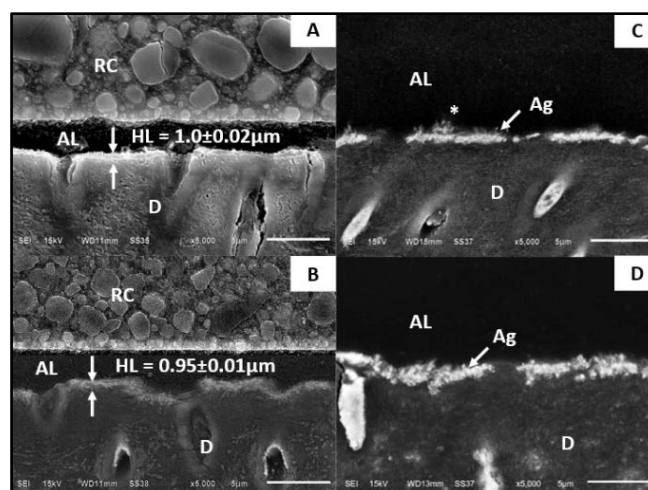


**Figure 7.** Resin-dentin interface of Single Bond Universal with simulated pulpal pressure. (A, C: immediate testing, B, D: 10,000-cycle thermocycling group. RC: resin composite, AL: adhesive layer, HL: hybrid layer, D: dentin, Ag: silver nitrate deposition, asterisk: water-tree phenomenon).

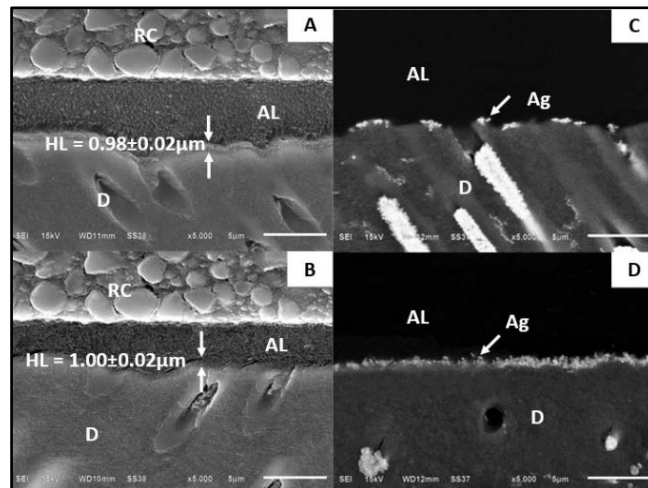


**Figure 8.** Resin-dentin interface of Single Bond Universal without simulated pulpal pressure. (A, C: immediate testing, B, D: 10,000-cycle thermocycling group. RC: resin composite, AL: adhesive layer, HL: hybrid layer, D: dentin, Ag: silver nitrate deposition).

#### 4.4 Discussion

At present, a universal adhesive is the latest generation of dental adhesive that is invented to reduce clinical steps and can also be used with both direct and indirect restorations (Cardoso et al., 2011). Single Bond Universal is defined as a universal adhesive with HEMA, which is considered to be a hydrophilic component. Existing of HEMA causes water retention in the adhesive layer as it reduces water evaporation in the solvent and also creates the water channel for pulling water from the dentin into the adhesive layer, which is prone to be degraded by hydrolysis (Wang & Spencer, 2005; Ye, Wang, & Spencer, 2009).

The result of the immediate  $\mu$ TBS values obtained from simulated pulpal pressure groups might be relatively lower than both non-simulated pulpal pressure groups and previous studies (Ahmed et al., 2019; Chen et al., 2015; Munoz et al., 2014) which might be due to the hydraulic pressure device. This machine is used for imitating the clinical situation of physiologically intrapulpal pressure simulation that pushes the dentinal fluids throughout the hybrid and adhesive layers, resulting in hydrolysis and plasticization, endangering the long-term durability of resin–dentin interfaces (Perdigao, 2010). This might result in an increased amount of silver deposited within the resin-dentin interfaces in the groups of simulated pulpal pressure. Besides, the water-tree pattern of nanoleakage related to the permeability of the adhesive was observed only in the groups of simulated pulpal pressure. The negative effect of the simulated pulpal pressure on the resin-dentin interface did not only affect the bond strength but also the failure mode pattern. The simulated pulpal pressure might result in a change in the pattern of failure from adhesive failure at the adhesive-dentin composite interface of non-simulated groups to adhesive failure at the adhesive-resin interface of simulated groups.

Also, the aging process with 10,000-cycle thermocycling under the condition of 5 and 55°C with a dwell time of 20 s in each water bath and a transfer time of 5 s was used in this study. This condition might imitate in vivo physical aging of restorative materials by cyclic exposure to hot and cold temperatures in a water bath that corresponds to 1-year physical aging in the oral cavity (El-Araby & Talic, 2007; Ernst, Canbek, Euler, & Willershausen, 2004). The stress that occurred at the resin-dentin interface associates with different thermal contraction/expansion coefficients between the restorative materials and tooth structure (Cenci et al., 2008). It accelerates the hydrolysis of demineralized collagen and extracts poorly polymerized resin oligomers by hot water, which endangered the microtensile bond strength (Ernst et al., 2004). In the same direction with this study, both ST and NT groups demonstrated statistically significant lower  $\mu$ TBS than the SI and NI, which were immediate testing groups ( $p < 0.05$ ). Thus, an increase in silver deposition within





the resin-dentin interfaces in the groups with thermocycling was observed. This confirmed the deleterious effect of thermal aging on the degradation of the resin-dentin interfaces.

Therefore, all null hypotheses in this study were rejected. There was a significance in microtensile bond strengths that were affected by the bonding process under simulated pulpal pressure and aging process ( $p < 0.01$ ).

Furthermore, another interesting topic that may be recommended for further study regarding the universal adhesive is the remaining solvent after the evaporating process of dentin bonding, which may be affected by the evaporating time, leading to compromised mechanical properties of the resin-dentin interfaces.

## 5. Conclusion

In conclusion, the  $\mu$ TBS value and nanoleakage of the resin-dentin interface could be affected by simulated pulpal pressure and 10,000 cycle thermocycling process. To avoid endangering the bond strength, besides controlling the environmental moisture, clinicians should pay attention to controlling the intrinsic moisture of the dentin surfaces.

## 6. Acknowledgements

Major advisor : Assoc.Prof. Dr.Pisol Senawongse

Co-advisor : Asst.Prof. Dr.Pipop Saikaew

Equipments : Research Center, Faculty of Dentistry, Mahidol university

## 7. References

- Ahmed, M. H., De Munck, J., Van Landuyt, K., Peumans, M., Yoshihara, K., & Van Meerbeek, B. (2019). Do Universal Adhesives Benefit from an Extra Bonding Layer? *J Adhes Dent*, *21*(2), 117-132. doi:10.3290/j.jad.a42304
- Armstrong, S., Breschi, L., Ozcan, M., Pfefferkorn, F., Ferrari, M., & Van Meerbeek, B. (2017). Academy of Dental Materials guidance on in vitro testing of dental composite bonding effectiveness to dentin/enamel using micro-tensile bond strength ( $\mu$ TBS) approach. *Dent Mater*, *33*(2), 133-143. doi:10.1016/j.dental.2016.11.015
- Arsathong K., T. C., Thitthaweerat S., Senawongs P. (2020). Effect of different methods for creating smear layer on fluid movement across resin/dentin interfaces created by a current self-etching adhesive. *M Dent J*, *40*(2), 8.
- Cardoso, M. V., de Almeida Neves, A., Mine, A., Coutinho, E., Van Landuyt, K., De Munck, J., & Van Meerbeek, B. (2011). Current aspects on bonding effectiveness and stability in adhesive dentistry. *Aust Dent J*, *56 Suppl 1*, 31-44. doi:10.1111/j.1834-7819.2011.01294.x
- Chen, C., Niu, L. N., Xie, H., Zhang, Z. Y., Zhou, L. Q., Jiao, K., . . . Tay, F. R. (2015). Bonding of universal adhesives to dentine--Old wine in new bottles? *J Dent*, *43*(5), 525-536. doi:10.1016/j.jdent.2015.03.004
- Ciucchi, B., Bouillaguet, S., Holz, J., & Pashley, D. (1995). Dentinal fluid dynamics in human teeth, in vivo. *J Endod*, *21*(4), 191-194. doi:10.1016/S0099-2399(06)80564-9
- do Amaral, R. C., Stanislawczuk, R., Zander-Grande, C., Michel, M. D., Reis, A., & Loguercio, A. D. (2009). Active application improves the bonding performance of self-etch adhesives to dentin. *J Dent*, *37*(1), 82-90. doi:10.1016/j.jdent.2008.09.010
- El-Araby, A. M., & Talic, Y. F. (2007). The effect of thermocycling on the adhesion of self-etching adhesives on dental enamel and dentin. *J Contemp Dent Pract*, *8*(2), 17-24. Retrieved from <https://www.ncbi.nlm.nih.gov/pubmed/17277823>
- Ernst, C. P., Canbek, K., Euler, T., & Willershausen, B. (2004). In vivo validation of the historical in vitro thermocycling temperature range for dental materials testing. *Clin Oral Investig*, *8*(3), 130-138. doi:10.1007/s00784-004-0267-2
- Ferrari, M., Goracci, C., Sadek, F., Eduardo, P., & Cardoso, C. (2002). Microtensile bond strength tests: scanning electron microscopy evaluation of sample integrity before testing. *Eur J Oral Sci*, *110*(5), 385-391. Retrieved from <https://www.ncbi.nlm.nih.gov/pubmed/12664470>
- Flury, S., Peutzfeldt, A., & Lussi, A. (2014). Influence of increment thickness on microhardness and dentin bond strength of bulk fill resin composites. *Dent Mater*, *30*(10), 1104-1112. doi:10.1016/j.dental.2014.07.001



- Hosaka, K., Nakajima, M., Yamauti, M., Aksornmuang, J., Ikeda, M., Foxton, R. M., . . . Tagami, J. (2007). Effect of simulated pulpal pressure on all-in-one adhesive bond strengths to dentine. *J Dent*, 35(3), 207-213. doi:10.1016/j.jdent.2006.08.001
- Munoz, M. A., Sezinando, A., Luque-Martinez, I., Szesz, A. L., Reis, A., Loguercio, A. D., . . . Perdigao, J. (2014). Influence of a hydrophobic resin coating on the bonding efficacy of three universal adhesives. *J Dent*, 42(5), 595-602. doi:10.1016/j.jdent.2014.01.013
- Nikaido, T., Kunzelmann, K. H., Chen, H., Ogata, M., Harada, N., Yamaguchi, S., . . . Tagami, J. (2002). Evaluation of thermal cycling and mechanical loading on bond strength of a self-etching primer system to dentin. *Dent Mater*, 18(3), 269-275. Retrieved from <https://www.ncbi.nlm.nih.gov/pubmed/11823020>
- Niyomsujarit, N., Senawongse, P., & Harnirattisai, C. (2019). Bond strength of self-etching adhesives to dentin surface after smear layer removal with ultrasonic brushing. *Dent Mater J*, 38(2), 287-294. doi:10.4012/dmj.2017-333
- Oilo, G. (1993). Bond strength testing--what does it mean? *Int Dent J*, 43(5), 492-498. Retrieved from <https://www.ncbi.nlm.nih.gov/pubmed/8138312>
- Pashley, D. H., & Tay, F. R. (2001). Aggressiveness of contemporary self-etching adhesives. Part II: etching effects on unground enamel. *Dent Mater*, 17(5), 430-444. Retrieved from <https://www.ncbi.nlm.nih.gov/pubmed/11445211>
- Perdigao, J. (2010). Dentin bonding-variables related to the clinical situation and the substrate treatment. *Dent Mater*, 26(2), e24-37. doi:10.1016/j.dental.2009.11.149
- Rosa, W. L., Piva, E., & Silva, A. F. (2015). Bond strength of universal adhesives: A systematic review and meta-analysis. *J Dent*, 43(7), 765-776. doi:10.1016/j.jdent.2015.04.003
- Saikaew, P., Matsumoto, M., Chowdhury, A., Carvalho, R. M., & Sano, H. (2018). Does Shortened Application Time Affect Long-Term Bond Strength of Universal Adhesives to Dentin? *Oper Dent*, 43(5), 549-558. doi:10.2341/17-205-L
- Sauro, S., Pashley, D. H., Montanari, M., Chersoni, S., Carvalho, R. M., Toledano, M., . . . Prati, C. (2007). Effect of simulated pulpal pressure on dentin permeability and adhesion of self-etch adhesives. *Dent Mater*, 23(6), 705-713. doi:10.1016/j.dental.2006.06.010
- Senawongse, P., Srihanon, A., Muangmingsuk, A., & Harnirattisai, C. (2010). Effect of dentine smear layer on the performance of self-etching adhesive systems: A micro-tensile bond strength study. *J Biomed Mater Res B Appl Biomater*, 94(1), 212-221. doi:10.1002/jbm.b.31643
- Shafiei, F., Kiomarsi, N., & Alavi, A. A. (2011). The effect of delayed placement of composite and double application of single-bottle adhesives on microleakage of composite restorations. *Gen Dent*, 59(1), 40-45; quiz 46-47, 80. Retrieved from <https://www.ncbi.nlm.nih.gov/pubmed/21613038>
- Sofan, E., Sofan, A., Palaia, G., Tenore, G., Romeo, U., & Migliau, G. (2017). Classification review of dental adhesive systems: from the IV generation to the universal type. *Ann Stomatol (Roma)*, 8(1), 1-17. doi:10.11138/ads/2017.8.1.001
- Tay, F. R., Pashley, D. H., Yiu, C. K., Sanares, A. M., & Wei, S. H. (2003). Factors contributing to the incompatibility between simplified-step adhesives and chemically-cured or dual-cured composites. Part I. Single-step self-etching adhesive. *J Adhes Dent*, 5(1), 27-40. Retrieved from <https://www.ncbi.nlm.nih.gov/pubmed/12729081>
- Van Landuyt, K. L., Snauwaert, J., De Munck, J., Peumans, M., Yoshida, Y., Poitevin, A., . . . Van Meerbeek, B. (2007). Systematic review of the chemical composition of contemporary dental adhesives. *Biomaterials*, 28(26), 3757-3785. doi:10.1016/j.biomaterials.2007.04.044
- Vongphan, N., Senawongse, P., Somsiri, W., & Harnirattisai, C. (2005). Effects of sodium ascorbate on microtensile bond strength of total-etching adhesive system to NaOCl treated dentine. *J Dent*, 33(8), 689-695. doi:10.1016/j.jdent.2005.01.008
- Wang, Y., & Spencer, P. (2005). Interfacial chemistry of class II composite restoration: structure analysis. *J Biomed Mater Res A*, 75(3), 580-587. doi:10.1002/jbm.a.30451
- Ye, Q., Wang, Y., & Spencer, P. (2009). Nanophase separation of polymers exposed to simulated bonding conditions. *J Biomed Mater Res B Appl Biomater*, 88(2), 339-348. doi:10.1002/jbm.b.31047